A Variant of Hoek's Æther-Drift Experiment

Kirk T. McDonald
Joseph Henry Laboratories, Princeton University, Princeton, NJ 08544
(May 14, 2023)

1 Problem

In the 1800's, many people sought an explanation of light as (transverse) vibrations in a mechanical medium, the luminiferous æther, that filled the Universe. A famous experiment of Fizeau [1, 2] found an effect in which water flowed in opposite directions in the two arms of an interferometer, who interpreted of this result as evidence for partial, but not complete, "dragging" of the æther in the apparatus.[1] This led to the experiment of Hoek [6] (sketched below, which had still water in one path of the "ring" interferometer, always at rest with respect to the Earth), that reported a null result (*i.e.*, no interference fringes at all, so the setup was defective in some way). Then, the famous Michelson-Morley experiment [7, 8, 9] observed interference fringes in a rotating interferometer (without water along any path), which fringes did not shift during the rotation, consistent with complete "dragging" of the æther in the apparatus, as well as the theory of special relativity [10].

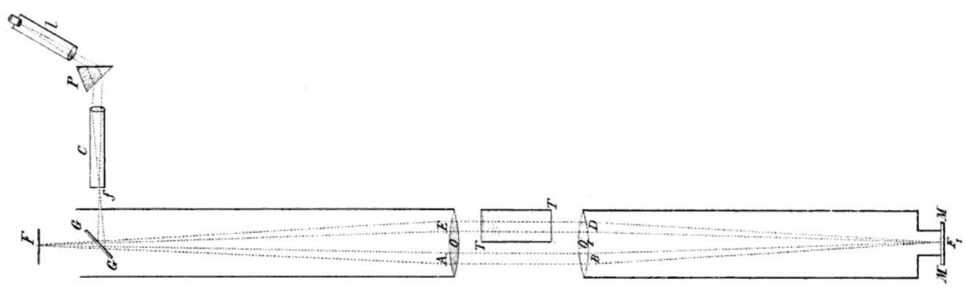

The laboratories of these experiments, on the surface of the Earth, were not strictly inertial frames (in which no effect would be expected according to special relativity). An effect of the rotation of the Earth was predicted by Michelson [11] (1904) in a "ring" interferometer where light propagated in both directions around the ring.[2] This prediction was elaborated upon by von Laue (1911)[13, 14]; see also [15]. An experiment by Michelson (1925) [16] with a ring interferometer of area roughly one square kilometer detected a small effect due to the rotation of the Earth, as consistent with special relativity.[3,4]

A key aspect of Hoek's interferometer (and also Fizeau's), with a dielectric medium in one path, is that effects of velocity are first order, rather than second order, as in interferometers whose paths are in air/vacuum.

Consider the interferometer sketched on the next page, in the frame of reference of the

[1]Discussions of complexities in Fizeau's experiment are given, for example, in [3, 4, 5].

[2]An early discussion of possible effects due to the motion of the Earth is sec. 76 of [12].

[3]Some discussion of Michelson's 1925 experiment is given in Appendix A.1.4 below.

[4]Ring interferometers exhibit a phase shift in their fringe pattern, when rotating about an axis perpendicular to the plane of the interferometer, compared to the pattern for no rotation. This effect was observed in table-top experiments "accidently" by Harress [17, 18, 19] (1911), and then "on purpose" by Sagnac [20, 21, 22] (1913). Reviews of the Sagnac effect include [23, 24].

Sun, approximating that frame as inertial. For simplicity, suppose the Earth's orbit is a circle of radius R, and that the axis of the Earth is not tilted with respect to the plane of its orbit about the Sun. The center of the interferometer is at latitude θ in, say, the northern hemisphere. The optical paths in the rectangle of the interferometer have lengths h and l, and one of the paths of length l has a glass block of length $L < l$ and index of refraction n. The interferometer is driven by a laser of wavelength λ (in air).

Deduce the phase differences $\Delta\phi_{12}$ and $\Delta\phi_{34}$ between the beams of light at beam splitter BS1 and splitter BS2 along the two paths 1-2 and 3-4. The difference of these differences characterizes the pattern of fringes that can be observed on the screen.

If the interferometer is rotated (quickly) about its center by 180°, as in the lower sketch below, the fringe pattern will shift by the difference of differences computed above.

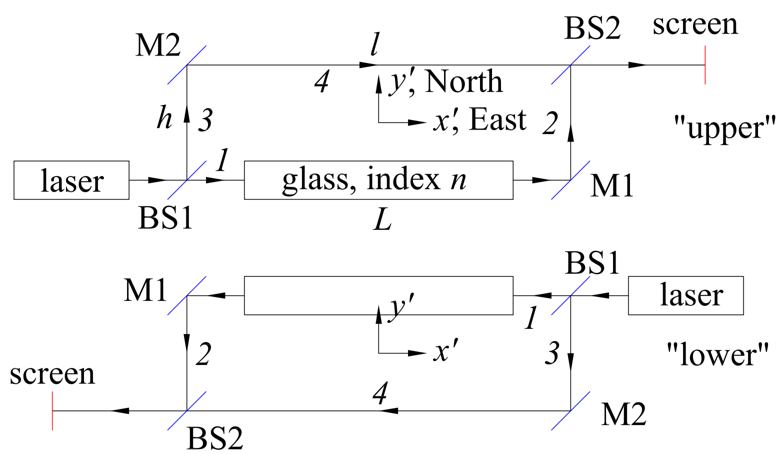

In addition to the (approximately) inertial frame of the Sun, we consider an accelerated (x', y', z') coordinate system fixed to the Earth, with x' to the East, y' to the North, and z' vertical, with its origin at the center of the interferometer.

It suffices to calculate only to first order in the velocities of elements of the interferometer, such that the Lorentz contraction of the interferometer, as observed in the frame of the Sun, can be ignored. Also, in the accelerated (x', y', z') frame the paths of the light between the various mirrors are slightly curved, but can be approximated as straight to first order in velocity.

This analysis is equivalent to assuming that the Sun is at rest in a classic æther, in which the speed of light is c in all directions. That is, experiments of the type of Hoek (and Sagnac; see [25]) do not distinguish between special relativity and an æther theory without "dragging" (in contrast to the experiment of Michelson and Morley [9], which is sensitive to second-order effects in velocity). Hence, the experiment of Hoek has seldom been repeated.

This note was inspired by e-discussions with An Rodriguez.

2 Solution

The analysis below compares various configurations of the interferometer at rest with respect to the surface of the Earth. In practice, the interferometer is in steady rotation, with respect to the Earth, about a vertical axis through its center, which leads to a phase shift between the two beams at the output of splitter BS2. This phase shift is independent of the orientation of the interferometer, and so does not affect the comparisons below, where it is neglected.[5]

We assume that the lengths of path segments 1 and 4 in the sketches above are the same, namely l, although this was not necessarily true in the 1925 experiment of Michelson [16], as mentioned in footnote 8 below.

The speed of light in vacuum/air is c (in all directions) in any inertial frame. This applies to the approximation, used here, that the rest frame of the Sun is inertial.

The velocity v of the center of the interferometer in the inertial frame of the Sun is,

$$v = \Omega R \cos \omega t + \omega r \cos \theta, \tag{1}$$

where the center of the interferometer is at latitude θ and distance r from the center of the Earth. Here, Ω is the angular velocity of the Earth in its (approximately circular) orbit about the Sun, ω is the angular velocity of the Earth about its axis,[6] and the factor $\cos \omega t$ refers to solar time with $t = 0$ at the local midnight at the interferometer.

For more detailed analysis of the interferometer, we consider only two configurations of it, the upper and lower sketched on the previous page. These two configurations differ by a rotation of 180° about the center of the interferometer. For both configurations we use a local coordinate system with the x'-axis pointing east and the y'-axis pointing north.

2.1 "Upper" Configuration

The velocities of path segments 1 and 4 (in the inertial frame of the Sun) are in the x' direction, and differ slightly from eq. (1). For the "upper" configuration, these velocities have the forms,

$$v_1 = \Omega R \cos \omega t + \omega r \cos(\theta - h/2r) \approx \Omega R \cos \omega t + \omega r \left(\cos \theta + \frac{h}{2r} \sin \theta \right), \tag{2}$$

$$v_4 = \Omega R \cos \omega t + \omega r \cos(\theta + h/2r) \approx \Omega R \cos \omega t + \omega r \left(\cos \theta - \frac{h}{2r} \sin \theta \right). \tag{3}$$

The speed of light, with respect to the frame of the Sun, that travels in the $\pm x'$ direction inside the (moving) glass block is,

$$c'_1 = \frac{c \mp n v_1}{n \mp v_1/c} \approx \frac{c}{n} \tag{4}$$

using eq. (25) of [26]. That is, corrections to the speed, c/n, of light inside a medium with index n at rest (in an inertial frame) are second-order in the velocity of the medium.

We now want to compute the phases of the two waves, that travel along paths 1-2 and 3-4, at beam splitter BS2 at time $t = 0$, relative to their common phase at splitter BS1 at time $t = 0$.[7] Recall that as a plane wave of form $e^{i(\mathbf{k}\cdot\mathbf{x} - \varpi t)}$, where ϖ/k is the wave speed, propagates from one spacetime point to another its phase $\phi = \mathbf{k} \cdot \mathbf{x} - \varpi t$ does not change. Hence, the phases we desire at splitter BS2 at time $t = 0$ are the same as those of the waves at the earlier time when they passed through splitter BS1.

[5] This phase shift was important in the 1925 experiment of Michelson [16], where the giant interferometer was at rest with respect to the (rotating) Earth, as discussed in Appendix A.1.4 below.

[6] $\Omega R \approx 10^{-4} c \approx 67\, \omega r$, while $\omega \approx 365\, \Omega$.

[7] Each of the two paths involves two reflections to reach the output side of splitter BS1 from the input side of splitter BS1. Since a 180° phase change occurs at each reflection, these phase changes are 360° on

2.1.1 Path 3-4

We first consider path 3-4 for the "upper" configuration of the interferometer in the figure on p. 2. Segment 3 is in motion in the x'-direction, so the path of light between the first beam splitter and the mirror is slightly tilted with respect to the y' axis and the optical path length is slightly longer than h. However, this effect is of second order in the velocity of the interferometer in the frame of the Sun, so we take the length of path 3 as approximately h. Then, the travel time of light along path 3 is approximately $\Delta t_3 = h/c$.

Segment 4 has x'-velocity (3) with respect to the frame of the Sun. The travel time Δt_4 along this path in the "upper" configuration of the interferometer is related by,

$$c\Delta t_4 = l + v_4 \Delta t_4, \qquad \Delta t_4 = \frac{l}{c - v_4} \approx \frac{l}{c}\left(1 + \frac{v_4}{c}\right). \tag{5}$$

The total travel time along path 3-4 is $\Delta t_3 + \Delta t_4$, so the light that arrived at the beam splitter BS1 at time $t = 0$ along path 3-4 left the splitter BS1 at time $-\Delta t_3 - \Delta t_4$, when splitter BS1 was at position $\Delta x' = -v_1(\Delta t_3 + \Delta t_4)$ relative to its position at $t = 0$. In the "upper" configuration the wave incident on splitter BS1 has the form $e^{i(kx' - \varpi t)}$, so the phase of the beam at this earlier position and time was, relative to the phase of the beam at splitter BS1 at time $t = 0$,

$$\begin{aligned}\Delta\phi_{34} = -kv_1(\Delta t_3 + \Delta t_4) + kc\,(\Delta t_3 + \Delta t_4) &= \frac{2\pi}{\lambda}\left(1 - \frac{v_1}{c}\right)\left[h + l\left(1 + \frac{v_4}{c}\right)\right] \\ &\approx \frac{2\pi}{\lambda}\left(h + l - \frac{v_1}{c}h + \frac{v_4 - v_1}{c}l\right).\end{aligned} \tag{6}$$

This is also the phase difference between the beam that arrived at splitter BS2 at time $t = 0$ along the path 3-4 and the phase of the beam at splitter BS1 at time $t = 0$.

2.1.2 Path 1-2

We now turn to the beam along path 1-2, which includes the glass block along segment 1.

The travel time along path segment 2 is the same as that along segment 3, so to first order in velocity, $\Delta t_2 = \Delta t_3 = h/c$.

The travel along segment 1 is in air for distance $l - L$ and in glass for distance L. Inside the latter, the speed of light along the x' axis in the inertial frame of the Sun is c/n to first order in the velocity of the glass block, as noted in eq. (4) above. Then, the travel time of light in segment 1 is, similarly to the argument of eq. (5) but with $v_4 \to v_1$,

$$\Delta t_1 \approx \frac{l - L}{c}\left(1 + \frac{v_1}{c}\right) + \frac{L}{c/n}\left(1 + \frac{v_1}{c/n}\right) = \frac{l - L}{c}\left(1 + \frac{v_1}{c}\right) + \frac{nL}{c}\left(1 + \frac{nv_1}{c}\right). \tag{7}$$

---

both paths, and can be ignored in the analysis.

There is also a 90° phase shift between the reflected and transmitted beams at a splitter. Since each of the two paths involves one reflection and one transmission at a splitter, there is no net phase difference in the two beam due to their passage through the splitters.

See, for example, Prob. 4 of [27].

And, similarly to eq. (6), the phase difference between the beam that arrived at splitter BS2 at time $t = 0$ along the path 1-2 and the phase of the beam at splitter BS1 at time $t = 0$ is,

$$\Delta\phi_{12} = k(c - v_1)(\Delta t_1 + \Delta t_2) = \frac{2\pi}{\lambda}\left(1 - \frac{v_1}{c}\right)\left[h + (l - L)\left(1 + \frac{v_1}{c}\right) + nL\left(1 + \frac{nv_1}{c}\right)\right]$$
$$\approx \frac{2\pi}{\lambda}\left(h + l + (n-1)L - \frac{v_1}{c}h + n(n-1)L\frac{v_1}{c}\right). \tag{8}$$

2.1.3 Difference of Phase Differences for the "Upper" Configuration

From eqs. (6) and (8) we have, for the "upper" configuration of the interferometer as sketched on p. 2,

$$\Delta\phi_{12} - \Delta\phi_{34} \approx \frac{2\pi}{\lambda}\left((n-1)L + n(n-1)L\frac{v_1}{c} + \frac{v_1 - v_4}{c}l\right)$$
$$\approx \frac{2\pi}{\lambda}\left\{(n-1)L + n(n-1)L\left[\frac{\Omega R}{c}\cos\omega t + \frac{\omega r}{c}\left(\cos\theta + \frac{h}{2r}\sin\theta\right)\right] + \frac{\omega hl\sin\theta}{c}\right\}, \tag{9}$$

recalling eqs. (2)-(3), with $t = 0$ at local midnight.

Even without the glass block, there is a term proportional to the angular velocity ω of rotation of the Earth about its axis and to the area hl of the interferometer. Such a term appears also in Sagnac-type interferometers.

The presence of the glass block leads to terms that depends both on the angular velocity Ω of the Earth in its orbit around the Sun and on the angular velocity ω.

2.1.4 Comparison of the "Upper" Configuration at Midnight and Noon

The difference (9) of phase differences implies a shift of the pattern of fringes observed on the screen of the interferometer, but a single observation does not provide a reference phase for the pattern. One way to extract information from the fringe pattern is to compare it for the same configuration of the interferometer ("upper" or "lower") at different times, such as midnight and noon (local time). A shift between these two observed fringe patterns for the "upper" configuration corresponds to, from eq. (9),

$$(\Delta\phi_{12} - \Delta\phi_{34})_{\rm midnight} - (\Delta\phi_{12} - \Delta\phi_{34})_{\rm noon} \approx \frac{4\pi}{\lambda}n(n-1)L\frac{\Omega R}{c}. \tag{10}$$

This effect is related only to the angular velocity Ω of the Earth about the Sun, and not to rotation of the Earth about its axis. It vanishes if the glass block is absent.

Since $\Omega R/c \approx 10^{-4}$ and $L/\lambda \approx 10^4$, this shift is of order an entire fringe.

2.2 "Lower" Configuration

For the "lower" configuration of the interferometer, as sketched on p. 2, the velocities of path segments 1 and 4 (in the inertial frame of the Sun) in the x'-direction have the forms,

$$v_1 = \Omega R\cos\omega t + \omega r\cos(\theta + h/2r) \approx \Omega R\cos\omega t + \omega r\left(\cos\theta - \frac{h}{2r}\sin\theta\right), \tag{11}$$

$$v_4 = \Omega R\cos\omega t + \omega r\cos(\theta - h/2r) \approx \Omega R\cos\omega t + \omega r\left(\cos\theta + \frac{h}{2r}\sin\theta\right), \tag{12}$$

which differ from eqs. (2)-(3) by the signs of the terms in path length h.

Again, the speed of light, with respect to the frame of the Sun, inside the glass block of index n is c/n, to first order in the velocity of the block.

2.2.1 Path 3-4

We now consider path 3-4 for the "lower" configuration of the interferometer in the figure on p. 2.

Again, the optical path length in (moving) segment 3 is affected by the motion only at second order in the velocity, so the travel time of light along path 3 is approximately $\Delta t_3 = h/c$.

Segment 4 has x'-velocity (12) with respect to the frame of the Sun, while the light in this segment travels in the $-x'$ direction in the "lower" configuration. The travel time Δt_4 along this path in the "lower" configuration of the interferometer is related by,

$$c\Delta t_4 = l - v_4 \Delta t_4, \qquad \Delta t_4 = \frac{l}{c + v_4} \approx \frac{l}{c}\left(1 - \frac{v_4}{c}\right). \tag{13}$$

The total travel time along path 3-4 is $\Delta t_3 + \Delta t_4$, so the light that arrived at the beam splitter BS2 at time $t = 0$ along path 3-4 left splitter BS1 at time $-\Delta t_3 - \Delta t_4$, when splitter BS1 was at position $\Delta x' = -v_1(\Delta t_3 + \Delta t_4)$ relative to its position at $t = 0$. In the "lower" configuration the wave incident on splitter BS1 has the form $e^{i(-kx' - \varpi t)}$ (taking the time dependence of the light to be $e^{-i\omega t}$ in both the "upper" and "lower" configurations), so the phase of the beam at this earlier position and time was, relative to the phase of the beam at splitter BS1 at time $t = 0$,

$$\begin{aligned}\Delta\phi_{34} = +kv_1(\Delta t_3 + \Delta t_4) + kc(\Delta t_3 + \Delta t_4) &= \frac{2\pi}{\lambda}\left(1 + \frac{v_1}{c}\right)\left[h + l\left(1 - \frac{v_4}{c}\right)\right] \\ &\approx \frac{2\pi}{\lambda}\left(h + l + \frac{v_1}{c}h + \frac{v_1 - v_4}{c}l\right).\end{aligned} \tag{14}$$

This is also the phase difference between the beam that arrived at splitter BS2 at time $t = 0$ along the path 3-4 and the phase of the beam at splitter BS1 at time $t = 0$.

2.2.2 Path 1-2

We now turn to the beam along path 1-2, which includes the glass block along segment 1.

The travel time along path segment 2 is the same as that along segment 3, so to first order in velocity, $\Delta t_2 = \Delta t_3 = h/c$.

The travel along segment 1 is partly in air and partly in glass. Inside the latter, the speed of light along the x' axis in the inertial frame of the Sun is c/n to first order in the velocity of the glass, as noted in eq. (4) above. Then, the travel time of light in segment 1 is, similarly to the argument of eq. (13),

$$\Delta t_1 \approx \frac{l - L}{c}\left(1 - \frac{v_1}{c}\right) + \frac{nL}{c}\left(1 - \frac{nv_1}{c}\right). \tag{15}$$

And, similarly to eq. (14), the phase difference between the beam that arrived at splitter BS2 at time $t = 0$ along the path 1-2 and the phase of the beam at splitter BS1 at time $t = 0$ is,

$$\Delta\phi_{12} = k(c + v_1)(\Delta t_1 + \Delta t_2) = \frac{2\pi}{\lambda}\left(1 + \frac{v_1}{c}\right)\left[h + (l - L)\left(1 - \frac{v_1}{c}\right) + nL\left(1 - \frac{nv_1}{c}\right)\right]$$
$$\approx \frac{2\pi}{\lambda}\left(h + l + (n-1)L + \frac{v_1}{c}h - n(n-1)L\frac{v_1}{c}\right). \qquad (16)$$

2.2.3 Difference of Phase Differences for the "Lower" Configuration

From eqs. (14) and (16) we have, for the "lower" configuration of the interferometer as sketched on p. 2,

$$\Delta\phi_{12} - \Delta\phi_{34} \approx \frac{2\pi}{\lambda}\left((n-1)L - n(n-1)L\frac{v_1}{c} - \frac{v_1 - v_4}{c}l\right)$$
$$\approx \frac{2\pi}{\lambda}\left\{(n-1)L - n(n-1)L\left[\frac{\Omega R\cos\omega t}{c} + \frac{\omega r}{c}\left(\cos\theta + \frac{h}{2r}\sin\theta\right)\right] - \frac{\omega hl\sin\theta}{c}\right\}, \qquad (17)$$

recalling eqs. (11)-(12).

2.2.4 Comparison of the "Lower" Configuration at Midnight and Noon

The difference (17) of phase differences implies a shift of the pattern of fringes observed on the screen of the interferometer, but a single observation does not provide a reference phase for the pattern. One way to extract information from the fringe pattern is to compare it for the "lower" configuration of the interferometer at midnight and noon (local time). A shift between these two observed fringe patterns corresponds to, from eq. (17),

$$(\Delta\phi_{12} - \Delta\phi_{34})_{\text{midnight}} - (\Delta\phi_{12} - \Delta\phi_{34})_{\text{noon}} \approx -\frac{4\pi}{\lambda}n(n-1)L\frac{\Omega R}{c}, \qquad (18)$$

which is the negative of that found in sec. 2.1.4 above.

2.2.5 Comparison of the "Upper" and "Lower" Configurations

We can also consider a comparison between the fringe patterns observed with the "upper" and "lower" configurations, by mounting the interferometer on a rotating platform. Then, the comparison between the "lower" configuration with the "upper" configuration one-half rotation apart in time is, from eqs. (9) and (17),

$$(\Delta\phi_{12} - \Delta\phi_{34})_{\text{upper}} - (\Delta\phi_{12} - \Delta\phi_{34})_{\text{lower}} \approx$$
$$\frac{4\pi}{\lambda}\left\{n(n-1)L\left[\frac{\Omega R\cos\omega t}{c} + \frac{\omega r}{c}\left(\cos\theta + \frac{h}{2r}\sin\theta\right)\right] + \frac{\omega hl\sin\theta}{c}\right\}$$
$$\approx \frac{4\pi}{\lambda}n(n-1)L\left(\frac{\Omega R}{c}\cos\omega t + \frac{\omega r\cos\theta}{c}\right). \qquad (19)$$

Since $L/\lambda \approx 10^4$ for a "table-top" interferometer and $\Omega R/c \approx 10^{-4}$, the shift of the fringe pattern every half rotation at midnight or noon (local time) is of order 1 fringe, while at 6 am and 9 pm the shift is only about 1/70 fringe (recalling that $\omega r \approx \Omega R/70$.

A Appendix: Analysis for Hoek's Original Experiment

Hoek's original experiment [6] involved propagation of light in both clockwise (CW) and counter-clockwise (CCW) senses using a single beam splitter and three mirrors, as sketched below. This is a "ring" interferometer configuration, and the interferometer has nonzero angular velocity due to the rotation of the Earth, even though it was fixed with respect to the Earth. In a sense, Hoek's experiment was a precursor of Sagnac's [22].

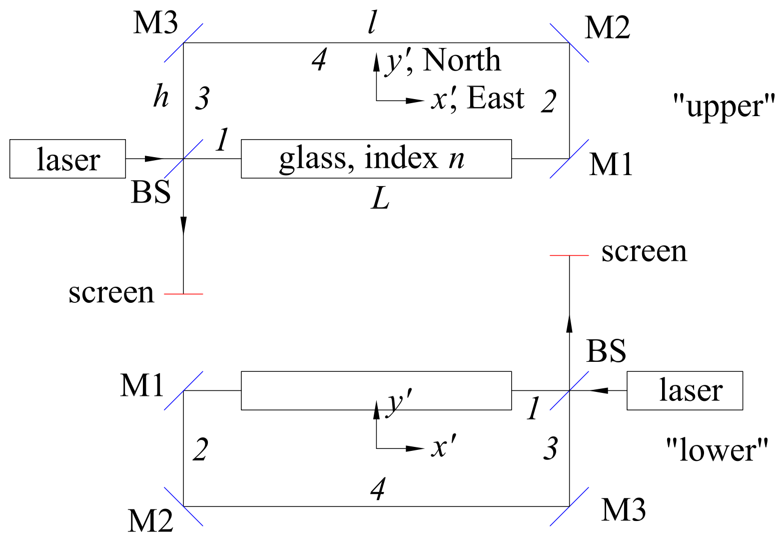

We want to compute the phase difference at time $t = 0$ between the clockwise and counter-clockwise beams at the final output side of the beam splitter, relative to their common phase at the input side of the beam splitter at $t = 0$. We will do this for both the "upper" and "lower" configurations shown above, although Hoek used only a single configuration, say, the "upper" one.

The clockwise path involves two reflections off the beam splitter and three reflections off the mirrors, while the counter-clockwise path involves two transmissions through the beam splitter, and three reflections off the mirror. This results in a 180° phase difference between the two beams in their final path to the screen that will be ignored in the following.

A.1 "Upper" Configuration

In the "upper" configuration of the interferometer sketched above, the velocities of path segments 1 and 4 have the same forms as in sec. 2.1 above,

$$v_{1,\text{up}} = \Omega R \cos \omega t + \omega r \cos(\theta - h/2r) \approx \Omega R \cos \omega t + \omega r \left(\cos \theta + \frac{h}{2r} \sin \theta \right), \tag{20}$$

$$v_{4,\text{up}} = \Omega R \cos \omega t + \omega r \cos(\theta + h/2r) \approx \Omega R \cos \omega t + \omega r \left(\cos \theta - \frac{h}{2r} \sin \theta \right). \tag{21}$$

As before, $t = 0$ at (local) midnight.

A.1.1 Counter-Clockwise Beam

A.1.1.1 Paths 2 and 3

As discussed in sec. 2.1.1 above, the transit times of light along paths 2 and 3 are just $\Delta t_2 = \Delta t_3 \approx h/c$ to first order in velocity, for both clockwise and counter-clockwise propagation.

A.1.1.2 Path 4

In the "upper" configuration, segment 4 has x'-velocity (21) with respect to the frame of the Sun. For counter-clockwise propagation, the travel time $\Delta t_{4,\mathrm{CCW}}$ along this path in the "upper" configuration of the interferometer is related by,

$$c\Delta t_{4,\mathrm{CCW}} = l - v_{4,\mathrm{up}}\Delta t_{4,\mathrm{CCW}}, \qquad \Delta t_{4,\mathrm{CCW}} = \frac{l}{c + v_{4,\mathrm{up}}} \approx \frac{l}{c}\left(1 - \frac{v_{4,\mathrm{up}}}{c}\right). \tag{22}$$

A.1.1.3 Path 1

In the "upper" configuration, segment 1 has x'-velocity (20) with respect to the frame of the Sun. Travel along this path is partly in air and partly in glass, so the time $\Delta t_{1,\mathrm{CCW}}$ along this path in the "upper" configuration of the interferometer is related by,

$$\Delta t_{1,\mathrm{CCW}} \approx \frac{l-L}{c}\left(1 + \frac{v_{1,\mathrm{up}}}{c}\right) + \frac{nL}{c}\left(1 + \frac{nv_{1,\mathrm{up}}}{c}\right), \tag{23}$$

as in eq. (7).

A.1.1.4 Δt_{CCW} and $\Delta\phi_{\mathrm{CCW}}$

The total travel time for counter-clockwise propagation is $\Delta t_{\mathrm{CCW}} = \Delta t_{1,\mathrm{CCW}} + \Delta t_2 + \Delta t_3 + \Delta t_{4,\mathrm{CCW}}$, so the light that arrived at the beam splitter at $t = 0$ after a round trip started from the beam splitter at time $t = -\Delta t_{\mathrm{CCW}}$, when the splitter was at position $\Delta x' = -v_{1,\mathrm{up}}\Delta t_{\mathrm{CCW}}$. In the "upper" configuration the wave incident on splitter BS1 has the form $e^{i(kx'-\varpi t)}$, so the phase of the beam at this earlier position and time was, relative to the phase of the beam at splitter at time $t = 0$,

$$\begin{aligned} \Delta\phi_{\mathrm{CCW}} &= -kv_{1,\mathrm{up}}\Delta t_{\mathrm{CCW}} + kc\,\Delta t_{CCW} \\ = \frac{2\pi}{\lambda}\left(1 - \frac{v_{1,\mathrm{up}}}{c}\right)&\left[2h + l\left(1 - \frac{v_{4,\mathrm{up}}}{c}\right) + (l-L)\left(1 + \frac{v_{1,\mathrm{up}}}{c}\right) + nL\left(1 + \frac{nv_{1,\mathrm{up}}}{c}\right)\right] \\ &\approx \frac{2\pi}{\lambda}\left(2h + 2l + (n-1)L - \frac{v_{1,\mathrm{up}}}{c}2h - \frac{v_{1,\mathrm{up}} + v_{4,\mathrm{up}}}{c}l + n(n-1)\frac{v_{1,\mathrm{up}}}{c}L\right). \end{aligned} \tag{24}$$

This is also the phase difference between the beam that arrived at splitter BS at time $t = 0$ after a round trip and the phase of the incident beam at splitter BS at time $t = 0$.

A.1.2 Clockwise Beam

A.1.2.1 Paths 2 and 3

Again, the transit times of light along paths 2 and 3 are just $\Delta t_2 = \Delta t_3 \approx h/c$ to first order in velocity, for both clockwise and counter-clockwise propagation.

A.1.2.2 Path 4

Clockwise propagation along segment 4 in the "upper" configuration has the same form as that in sec. 2.2.1 above (but with v_4 given by eq. (21); and also eq. (22) with sith sign of v_4 reversed),

$$\Delta t_{4,\mathrm{up}} \approx \frac{l}{c}\left(1 + \frac{v_{4,\mathrm{up}}}{c}\right). \tag{25}$$

A.1.2.3 Path 1

Segment 1 has x'-velocity (20) with respect to the frame of the Sun. For clockwise propagation, the time $\Delta t_{1,\mathrm{CW}}$ along this path in the "upper" configuration of the interferometer is related by,

$$\Delta t_{1,\mathrm{CW}} \approx \frac{l-L}{c}\left(1 - \frac{v_{1,\mathrm{up}}}{c}\right) + \frac{nL}{c}\left(1 - \frac{nv_{1,\mathrm{up}}}{c}\right), \tag{26}$$

which is that of eq. (23) with the sign of $v_{1,\mathrm{up}}$ reversed.

A.1.2.4 Δt_{CW} and $\Delta\phi_{\mathrm{CW}}$

The total travel time for clockwise propagation is $\Delta t_{\mathrm{CW}} = \Delta t_{1,\mathrm{CW}} + \Delta t_2 + \Delta t_3 + \Delta t_{4,\mathrm{CW}}$, so the light that arrived at the beam splitter at $t = 0$ after a round trip started from the beam splitter at time $t = -\Delta t_{\mathrm{CW}}$, when the splitter was at position $\Delta x' = -v_{1,\mathrm{up}}\Delta t_{\mathrm{CW}}$. In the "upper" configuration the wave incident on splitter BS1 has the form $e^{i(kx'-\varpi t)}$, so the phase of the beam at this earlier position and time was, relative to the phase of the beam at splitter at time $t = 0$,

$$\begin{aligned} \Delta\phi_{\mathrm{CW}} &= -kv_{1,\mathrm{up}}\Delta t_{\mathrm{CW}} + kc\,\Delta t_{CW} \\ = \frac{2\pi}{\lambda}\left(1 - \frac{v_{1,\mathrm{up}}}{c}\right)&\left[2h + l\left(1 + \frac{v_{4,\mathrm{up}}}{c}\right) + (l-L)\left(1 - \frac{v_{1,\mathrm{up}}}{c}\right) + nL\left(1 - \frac{nv_{1,\mathrm{up}}}{c}\right)\right] \\ &\approx \frac{2\pi}{\lambda}\left(2h + 2l + (n-1)L - \frac{v_{1,\mathrm{up}}}{c}2h + \frac{v_{4,\mathrm{up}} - 3v_{1,\mathrm{up}}}{c}l - n(n-1)\frac{v_{1,\mathrm{up}}}{c}L\right). \end{aligned} \tag{27}$$

This is also the phase difference between the beam that arrived at splitter BS at time $t = 0$ after a round trip and the phase of the incident beam at splitter BS at time $t = 0$.

A.1.3 $\Delta\phi_{\mathrm{CCW}} - \Delta\phi_{\mathrm{CW}}$

The phase difference between the counter-clockwise and clockwise beams at the output side of the beam splitter in the "upper" configuration is, from eqs. (24) and (27),recalling eqs. (20)-(21),

$$\begin{aligned} \Delta\phi_{\mathrm{CCW}} - \Delta\phi_{\mathrm{CW}} &\approx \frac{2\pi}{\lambda}\left(\frac{2v_{1,\mathrm{up}} - 2v_{4,\mathrm{up}}}{c}l + 2n(n-1)\frac{v_{1,\mathrm{up}}}{c}L\right) \\ \approx \frac{2\pi}{\lambda}&\left\{\frac{2\omega r}{c}\frac{hl\sin\theta}{r} + 2n(n-1)\left[\frac{\Omega R\cos\omega t}{c} + \frac{\omega r}{c}\left(\cos\theta + \frac{h}{2r}\sin\theta\right)\right]L\right\}. \end{aligned} \tag{28}$$

A.1.4 Michelson's Experiment of 1925

The effect of eq. (28) was studied by Michelson in 1925 [16] without any glass block, via a very large, fixed interferometer in, say, the "upper" configuration sketched on p. 8 above. Michelson compared the phase shift between counterpropagating beams in the very large interferometer to that at the same time in a much smaller interferometer driven by the same light source.

In this case, the interferometer(s) are rotating at angular velocity $(\omega + \Omega)\sin\theta \approx \omega\sin\theta$ about their centers. Our analysis has neglected this effect on path segments 2 and 3, as it is not relevant for comparison of the fringe pattern of a rotating interferometer at different times. An analysis including this rotation was given by Silberstein [15], valid for any interferometer in air/vacuum with any number of straight path segments, finding, for area vector $\mathbf{A}$, of magnitude hl, that points along the local vertical at the interferometer,[8]

$$\Delta\phi_{\rm CCW} - \Delta\phi_{\rm CW} \approx \frac{8\pi}{\lambda}\frac{\omega hl\sin\theta}{c} = \frac{8\pi\,\boldsymbol{\omega}\cdot\mathbf{A}}{\lambda c} \tag{29}$$

which is twice the result of eq. (28) for $n = 1$.[9]

A.1.5 Comparison of the "Upper" Configuration at Midnight and Noon

The difference (28) of phase differences implies a shift of the pattern of fringes observed on the screen of the interferometer, but a single observation does not provide a reference phase for the pattern. One way to extract information from the fringe pattern is to compare it for the same configuration of the interferometer ("upper" or "lower") and midnight and noon (local time). A shift between these two observed fringe patterns corresponds to, from eq. (28),

$$(\Delta\phi_{\rm CCW} - \Delta_{\rm CW})_{\rm midnight} - (\Delta\phi_{\rm CCW} - \Delta_{\rm CW})_{\rm noon} \approx \frac{8\pi}{\lambda}n(n-1)L\frac{\Omega R}{c}\,. \tag{30}$$

As in sec. 2.1.4 above, this effect is related only to the angular velocity Ω of the Earth about the Sun, and not to the rotation of the Earth about its axis.

A.2 "Lower" Configuration

For the "lower" configuration of the interferometer as sketched on p. 8, the velocities of path segments 1 and 4 (in the inertial frame of the Sun) in the x'-direction have the forms,

$$v_{1,\rm lo} = \Omega R\cos\omega t + \omega r\cos(\theta + h/2r) \approx \Omega R\cos\omega t + \omega r\left(\cos\theta - \frac{h}{2r}\sin\theta\right), \tag{31}$$

$$v_{4,\rm lo} = \Omega R\cos\omega t + \omega r\cos(\theta - h/2r) \approx \Omega R\cos\omega t + \omega r\left(\cos\theta + \frac{h}{2r}\sin\theta\right). \tag{32}$$

[8]See also https://en.wikipedia.org/wiki/Sagnac_effect

[9]Michelson gave a derivation in [16] more like ours, considering only the rotation ω of the Earth about its axis, except that he supposed path segments 2 and 3 both pointed to the local North, converging slightly, such that segment 4 is shorter than segment 1. This indeed doubles the result of eq. (28) for $n = 1$, but is something of a "fake" derivation in that if the terms in ΩR were kept they would be quite large, rather than canceling for $n = 1$ as in eq. (28).

which differ from eqs. (20)-(21) by the signs of the terms in path length h.

A.2.1 Counter-Clockwise Beam

A.2.1.1 Paths 2 and 3

As discussed in sec. 2.1.1 above, the transit times of light along paths 2 and 3 are just $\Delta t_2 = \Delta t_3 \approx h/c$ to first order in velocity, for both clockwise and counter-clockwise propagation.

A.2.1.2 Path 4

In the "lower" configuration, segment 4 has x'-velocity (32) with respect to the frame of the Sun. For counter-clockwise propagation, the travel time $\Delta t_{4,\mathrm{CCW}}$ along this path in the "lower" configuration of the interferometer is related by,

$$c\Delta t_{4,\mathrm{CCW}} = l + v_{4,\mathrm{lo}}\Delta t_{4,\mathrm{CCW}}, \qquad \Delta t_{4,\mathrm{CCW}} = \frac{l}{c - v_{4,\mathrm{up}}} \approx \frac{l}{c}\left(1 + \frac{v_{4,\mathrm{lo}}}{c}\right). \tag{33}$$

A.2.1.3 Path 1

In the "lower" configuration, segment 1 has x'-velocity (31) with respect to the frame of the Sun. Travel along this path is partly in air and partly in glass, so the time $\Delta t_{1,\mathrm{CCW}}$ along this path in the "lower" configuration of the interferometer is related by,

$$\Delta t_{1,\mathrm{CCW}} \approx \frac{l-L}{c}\left(1 - \frac{v_{1,\mathrm{lo}}}{c}\right) + \frac{nL}{c}\left(1 - \frac{nv_{1,\mathrm{lo}}}{c}\right), \tag{34}$$

as in eq. (15).

A.2.1.4 Δt_{CCW} and $\Delta\phi_{\mathrm{CCW}}$

The total travel time for counter-clockwise propagation is $\Delta t_{\mathrm{CCW}} = \Delta t_{1,\mathrm{CCW}} + \Delta t_2 + \Delta t_3 + \Delta t_{4,\mathrm{CCW}}$, so the light that arrived at the beam splitter at $t = 0$ after a round trip started from the beam splitter at time $t = -\Delta t_{\mathrm{CCW}}$, when the splitter was at position $\Delta x' = -v_{1,\mathrm{lo}}\Delta t_{\mathrm{CCW}}$. In the "lower" configuration the wave incident on splitter BS1 has the form $e^{i(-kx'-\varpi t)}$, so the phase of the beam at this earlier position and time was, relative to the phase of the beam at splitter at time $t = 0$,

$$\begin{aligned} \Delta\phi_{\mathrm{CCW}} &= kv_{1,\mathrm{lo}}\Delta t_{\mathrm{CCW}} + kc\,\Delta t_{CCW} \\ = \frac{2\pi}{\lambda}\left(1 + \frac{v_{1,\mathrm{lo}}}{c}\right)&\left[2h + l\left(1 + \frac{v_{4,\mathrm{lo}}}{c}\right) + (l-L)\left(1 - \frac{v_{1,\mathrm{lo}}}{c}\right) + nL\left(1 - \frac{nv_{1,\mathrm{lo}}}{c}\right)\right] \\ &\approx \frac{2\pi}{\lambda}\left(2h + 2l + (n-1)L + \frac{v_{1,\mathrm{lo}}}{c}2h + \frac{v_{1,\mathrm{lo}} + v_{4,\mathrm{lo}}}{c}l - n(n-1)\frac{v_{1,\mathrm{lo}}}{c}L\right). \end{aligned} \tag{35}$$

This is also the phase difference between the beam that arrived at splitter BS at time $t = 0$ after a round trip and the phase of the incident beam at splitter BS at time $t = 0$.

A.2.2 Clockwise Beam

A.2.2.1 Paths 2 and 3

Again, the transit times of light along paths 2 and 3 are just $\Delta t_2 = \Delta t_3 \approx h/c$ to first order in velocity, for both clockwise and counter-clockwise propagation.

A.2.2.2 Path 4

Clockwise propagation along segment 4 in the "lower" configuration has the same form as that in sec. 2.2.1 above (but with v_4 given by eq. (32); and also eq. (33) with sith sign of v_4 reversed),

$$\Delta t_{4,\mathrm{lo}} \approx \frac{l}{c}\left(1 - \frac{v_{4,\mathrm{lo}}}{c}\right). \tag{36}$$

A.2.2.3 Path 1

Segment 1 has x'-velocity (31) with respect to the frame of the Sun. For clockwise propagation, the time $\Delta t_{1,\mathrm{CW}}$ along this path in the "lower" configuration of the interferometer is related by,

$$\Delta t_{1,\mathrm{CW}} \approx \frac{l-L}{c}\left(1 + \frac{v_{1,\mathrm{lo}}}{c}\right) + \frac{nL}{c}\left(1 + \frac{nv_{1,\mathrm{lo}}}{c}\right), \tag{37}$$

which is that of eq. (34) with the sign of $v_{1,\mathrm{lo}}$ reversed.

A.2.2.4 Δt_{CW} and $\Delta\phi_{\mathrm{CW}}$

The total travel time for clockwise propagation is $\Delta t_{\mathrm{CW}} = \Delta t_{1,\mathrm{CW}} + \Delta t_2 + \Delta t_3 + \Delta t_{4,\mathrm{CW}}$, so the light that arrived at the beam splitter at $t = 0$ after a round trip started from the beam splitter at time $t = -\Delta t_{\mathrm{CW}}$, when the splitter was at position $\Delta x' = -v_{1,\mathrm{lo}}\Delta t_{\mathrm{CW}}$. In the "lower" configuration the wave incident on splitter BS1 has the form $e^{i(-kx'-\varpi t)}$, so the phase of the beam at this earlier position and time was, relative to the phase of the beam at splitter at time $t = 0$,

$$\begin{aligned} \Delta\phi_{\mathrm{CW}} &= kv_{1,\mathrm{lo}}\Delta t_{\mathrm{CW}} + kc\,\Delta t_{CW} \\ = \frac{2\pi}{\lambda}\left(1 + \frac{v_{1,\mathrm{lo}}}{c}\right)\left[2h + l\left(1 - \frac{v_{4,\mathrm{lo}}}{c}\right) + (l-L)\left(1 + \frac{v_{1,\mathrm{lo}}}{c}\right) + nL\left(1 + \frac{nv_{1,\mathrm{lo}}}{c}\right)\right] & \\ \approx \frac{2\pi}{\lambda}\left(2h + 2l + (n-1)L + \frac{v_{1,\mathrm{lo}}}{c}2h + \frac{3v_{1,\mathrm{lo}} - v_{4,\mathrm{lo}}}{c}l + n(n-1)\frac{v_{1,\mathrm{lo}}}{c}L\right). & \end{aligned} \tag{38}$$

This is also the phase difference between the beam that arrived at splitter BS at time $t = 0$ after a round trip and the phase of the incident beam at splitter BS at time $t = 0$.

A.2.3 $\Delta\phi_{\mathrm{CCW}} - \Delta\phi_{\mathrm{CW}}$

The phase difference between the counter-clockwise and clockwise beams at the output side of the beam splitter in the "lower" configuration is, from eqs. (35) and (38), and recalling eqs. (31)-(32),

$$\Delta\phi_{\rm CCW} - \Delta\phi_{\rm CW} \approx \frac{2\pi}{\lambda}\left(\frac{2v_{4,\rm lo} - 2v_{1,\rm lo}}{c} l - 2n(n-1)\frac{v_{1,\rm lo}}{c} L\right) \tag{39}$$

$$\approx \frac{2\pi}{\lambda}\left\{\frac{2\omega r}{c}\frac{hl\sin\theta}{r} - 2n(n-1)\left[\frac{\Omega R\cos\omega t}{c} + \frac{\omega r}{c}\left(\cos\theta - \frac{h}{2r}\sin\theta\right)\right] L\right\}.$$

Again, the plus(minus) signs before ω apply at midnight(noon).

A.2.4 Comparison of the "Upper" and "Lower" Configurations

The difference (28) of phase differences implies a shift of the pattern of fringes observed on the screen of the interferometer, but a single observation does not provide a reference phase for the pattern. One way to extract information from the fringe pattern is to compare the "upper" and "lower" configurations of a rotating interferometer one-half turn apart. A shift between these two observed fringe patterns corresponds to, from eqs. (28) and (39),

$$(\Delta\phi_{\rm CCW} - \Delta_{\rm CW})_{\rm upper} - (\Delta\phi_{\rm CCW} - \Delta_{\rm CW})_{\rm lower} \approx \frac{8\pi}{\lambda} n(n-1) L\left(\frac{\Omega R\cos\omega t}{c} + \frac{\omega r}{c}\cos\theta\right). \tag{40}$$

This is double the result of eq. (19).

References

[1] M.H. Fizeau, *Sur les hypothèses relatives à l'éther lumineux, et sur une expérience qui parait démontrer que le mouvement des corps change la vitesse avec laquelle la lumière se propage dans leur intérieur*, Comptes Rend. Acad. Sci. **33**, 349 (1851), http://kirkmcd.princeton.edu/examples/GR/fizeau_cras_33_349_51.pdf
On the Hypotheses Relating to the Luminous Æther and an Experiment which appears to Demonstrate that the Motion of Bodies alters the Velocity with which Light propagates Itself in Their Interior, Phil. Mag. **2**, 568 (1851), http://kirkmcd.princeton.edu/examples/GR/fizeau_pm_2_568_51.pdf

[2] M.H. Fizeau, *Sur les hypothèses relatives à l'éther lumineux, et sur une expérience qui parait démontrer que le mouvement des corps change la vitesse avec laquelle la lumière se propage dans leur intérieur*, Ann. Chim. Phys. **57**, 385 (1859), http://kirkmcd.princeton.edu/examples/GR/fizeau_acp_57_385_59.pdf
On the Effect of the Motion of a Body upon the Velocity with which it is traversed by Light, Phil. Mag. **19**, 245 (1860), http://kirkmcd.princeton.edu/examples/GR/fizeau_pm_19_245_60.pdf

[3] R.J. Neutze, G.E. Stedman and H.R. Bilger, *Reanalysis of Laub drag effects in a ring cavity*, J. Opt. Soc. Am. B **13**, 2065 (1996), http://kirkmcd.princeton.edu/examples/GR/neutze_josab_13_2065_96.pdf

[4] I. Lerche, *The Fizeau effect: Theory, experiment, and the Zeeman's measurements*, Am. J. Phys **45**, 1154 (1977), http://kirkmcd.princeton.edu/examples/GR/lerche_ajp_45_1154_77.pdf

[5] G. Clément, *Does the Fizeau experiment really test special relativity?* Am. J. Phys **48**, 1059 (1980), http://kirkmcd.princeton.edu/examples/GR/clement_ajp_48_1059_180.pdf

[6] M. Hoek, *Determination de la vitesse avec laquelle est entrainée une onde lumineuse traversant un milieu en mouvement*, Arch. Neer. Acad. Sci. **3**, 180 (1868),
http://kirkmcd.princeton.edu/examples/GR/hoek_ans_3_180_68.pdf
http://kirkmcd.princeton.edu/examples/GR/hoek_vmkaw_2_189_68.pdf
http://kirkmcd.princeton.edu/examples/GR/hoek_vmkaw_2_189_68_english.pdf
http://kirkmcd.princeton.edu/examples/GR/hoek_69.pdf

[7] A.A. Michelson, *The relative motion of the Earth and the Luminifeous ether*, Am. J. Sci. **22**, 210 (1881). http://kirkmcd.princeton.edu/examples/GR/michelson_ajs_22_120_81.pdf

[8] A.A. Michelson and E. Morley, *Influence of the Motion of the Medium on the Velocity of Light*, Am. J. Sci. **31**, 377 (1886).
http://kirkmcd.princeton.edu/examples/GR/michelson_ajs_31_377_86.pdf

[9] A.A. Michelson and E. Morley, *On the Relative Motion of the Earth and the Luminiferous Ether*, Am. J. Sci. **34**, 333 (1887).
http://kirkmcd.princeton.edu/examples/GR/michelson_ajs_34_333_87.pdf
Phil. Mag. **24**, 499 (1997). http://kirkmcd.princeton.edu/examples/GR/michelson_pm_24_449_87.pdf

[10] A. Einstein, *Zur Elektrodynamik bewegter Körper*, Ann. d. Phys. **17**, 891 (1905),
http://kirkmcd.princeton.edu/examples/EM/einstein_ap_17_891_05.pdf
http://kirkmcd.princeton.edu/examples/EM/einstein_ap_17_891_05_english.pdf

[11] A.A. Michelson, *Relative Motion of Earth and Æther*, Phil. Mag. **8**, 716 (1904).
http://kirkmcd.princeton.edu/examples/GR/michelson_pm_8_716_04.pdf

[12] O. Lodge, *Aberration Problems: a Discussion concerning the Connexion between Ether and Matter, and the Motion of the Ether near the Earth*, Phil. Trans. Roy. Soc. London **184**, 727 (1893). http://kirkmcd.princeton.edu/examples/GR/lodge_ptrlsa_184_727_93.pdf

[13] M. von Laue, *Über einen Versuch zur Optik der bewegten Körper*, Münch. Sitz.-Ber. 401 (1911). http://kirkmcd.princeton.edu/examples/GR/vonlaue_ms_405_11.pdf
http://kirkmcd.princeton.edu/examples/GR/vonlaue_ms_405_11_english.pdf

[14] M. von Laue, *Zum Versuch von F. Harreβ*, Ann. d. Phys. **62**, 448 (1920).
http://kirkmcd.princeton.edu/examples/GR/vonlaue_ap_62_448_20.pdf
http://kirkmcd.princeton.edu/examples/GR/vonlaue_ap_62_448_20_english.pdf

[15] L. Silberstein, *The Propagation of Light in Rotating Systems*, J. Opt. Soc. Am. **5**, 291 (1921). http://kirkmcd.princeton.edu/examples/GR/silberstein_josa_5_291_21.pdf

[16] A.A. Michelson, *The Effect of the Earth's Rotation on the Velocity of Light*, Part I, Ap. J. **61**, 137 (1925). http://kirkmcd.princeton.edu/examples/GR/michelson_apj_61_137_25.pdf
with H.G. Gale, Part II, Ap. J. **61**, 140 (1925).
http://kirkmcd.princeton.edu/examples/GR/michelson_apj_61_140_25.pdf
Nature **115**, 566 (1925). http://kirkmcd.princeton.edu/examples/GR/michelson_nature_115_566_25.pdf

[17] O. Knopf, *Die Versuche von F. Harreß über die Qeschwindigkeit des Lichtes in bewegten Körper*, Ann. d. Phys. **62**, 389 (1920).
http://kirkmcd.princeton.edu/examples/GR/knopf_ap_62_389_20.pdf

[18] B. Pogány, *Über die Wiederholung des Harress-Sagnacschen Versuches*, Ann. d. Phys. **80**, 217 (1926). http://kirkmcd.princeton.edu/examples/GR/pogany_ap_80_217_26.pdf

[19] B. Pogány, *Über die Wiederholung des Harressschen Versuches*, Ann. d. Phys. **85**, 244 (1928). http://kirkmcd.princeton.edu/examples/GR/pogany_ap_85_244_28.pdf

[20] G. Sagnac, *L'éther lumineux démontré par l'effet du vent relatif d'éther dans un interféromètre en rotation uniforme*, Compte Rend. Acad. Sci. **157**, 708 (1913).
http://kirkmcd.princeton.edu/examples/GR/sagnac_cras_157_708_13.pdf
http://kirkmcd.princeton.edu/examples/GR/sagnac_cras_157_708_13_enlgish.pdf

[21] G. Sagnac, *Sur la preuve de la réalité de l'éther lumineux par l'expérience de l'interférographe tournant*, Compte Rend. Acad. Sci. **157**, 1410 (1913).
http://kirkmcd.princeton.edu/examples/GR/sagnac_cras_157_1410_13.pdf
http://kirkmcd.princeton.edu/examples/GR/sagnac_cras_157_1410_13_english.pdf

[22] G. Sagnac, *Effet tourbillonnaire optique. La circulation de l'éther lumineux dans un interférographe tournant*, J. Phys. **4**, 177 (1914).
http://kirkmcd.princeton.edu/examples/GR/sagnac_jp_4_177_14.pdf

[23] E.J. Post, *Sagnac Effect*, Rev. Mod. Phys. **39**, 475 (1967).
http://kirkmcd.princeton.edu/examples/GR/post_rmp_39_475_67.pdf

[24] R. Anderson, H.R. Bilger and G.E. Stedman, *"Sagnac" Effect: A century of earth-rotated inteferomoters*, Am. J. Phys. **62**, 975 (1994).
http://kirkmcd.princeton.edu/examples/GR/anderson_ajp_62_975_94.pdf

[25] K.Brown, *The Sagnac Effect*. https://www.mathpages.com/rr/s2-07/2-07.htm

[26] K.T. McDonald, *Index of Refraction of a Moving Medium* (Dec. 17, 2014).
http://kirkmcd.princeton.edu/examples/index.pdf

[27] K.T. McDonald, *Electrodynamics Problem Set 6* (2011).
http://kirkmcd.princeton.edu/examples/ph501set6.pdf